Available online at www.sciencedirect.com
ScienceDirect
Physics Letters A 363 (2007) 297–301
PHYSICS LETTERS A
www.elsevier.com/locate/pla

Dust diagnostics on an inertial electrostatic confinement discharge

Joe Khachan *, Alex Samarian

School of Physics, University of Sydney, Sydney 2006, Australia

Received 23 April 2006; received in revised form 4 October 2006; accepted 9 November 2006

Available online 15 November 2006

Communicated by F. Porcelli

Abstract

Micron size dust particles were used to diagnose the direction of ion flow in an inertial electrostatic confinement discharge. Particles were dropped onto a one-dimensional device and were shown to deflect away from the center. The deflection of the dust particles was then accounted for by ion drag. It is concluded that ions are created at the cathode center and flow outwards. This supports recent work that has reached the same conclusion using Doppler spectroscopy. Moreover, estimates of the ion density from the deflection of dust particles was in agreement with Langmuir probe measurements.

PACS: 52.27.Lw; 52.58.Qv; 52.70.-m; 52.80.-s

A concentric anode and cathode geometry has been used to produce energetic deuterium discharges that lead to a substantial number of nuclear fusion reactions. The cathode (inner electrode) consists of a spherical wire grid and is consequently highly transparent to ions. The basic idea is to create a deep electrostatic potential well in order to trap ions and confine them for a long enough time. For this reason, this concept has been called inertial electrostatic confinement (IEC) [1–5].

In reality, many IEC devices are operated in a gaseous discharge mode in the units to tens of mTorr pressure range [6]. As a result, atomic collision processes, such as charge exchange, dominate in such discharges. Moreover, the hydrogen IEC discharge used in this Letter has been shown [7] to consist of monoenergetic beams of H^+, H_2^+ and H_3^+ with $\approx 60\%$ H_2^+ at pressures in the order of tens of mTorr. However, this ratio changes slightly for a different hollow cathode type [8]. Typical energies of these ions have been shown [7] to be $\approx 30\%$ of the applied cathode potential. Langmuir probe measurements on the apparatus used for this Letter give plasma densities in the center in the order of 10^8 cm^{-3}. Double probe measurements in a larger IEC device [9] and operating at higher powers than ours was found to have plasma densities in the order of 10^9 cm^{-3}. The electron energy distribution has not been directly measured, however, we will assume in this work that their energy distribution is the same as those of the ions.

Despite the prominence of atomic collision effects, it has been demonstrated that nuclear fusion reactions rates in deuterium are typically $\sim 10^7$ s^{-1} for input powers of several hundred Watts (a factor of a 100 higher for a 50% tritium mixture) [6]. This is due to the collision of deuterium beams with the background gas [10] rather than beam–beam collisions.

To achieve the idealized concept of particle trapping by an electrostatic potential well, one must operate under ultra high vacuum conditions. As a result, it is of interest to determine the particle energy and their flow direction when such a device is operated in the gaseous discharge regime. Doppler shift spectroscopy [11] has shown that there is substantial ion flux created at the cathode center and accelerates outwards. They exit the cathode as neutrals because the atomic and molecular ions species (H^+, H_2^+ and H_3^+) undergo charge exchange with the background gas. Most of these molecular ion species fragment into atomic neutrals after charge exchange.

In this Letter we present measurements of the energy and direction of the energetic ions using falling dust particles as a diagnostic tool. Particles were dropped onto an IEC device and were shown to deflect away from the center of the cathode. An

* Corresponding author.
E-mail address: j.khachan@physics.usyd.edu.au (J. Khachan).

0375-9601/$ – see front matter
doi:10.1016/j.physleta.2006.11.015

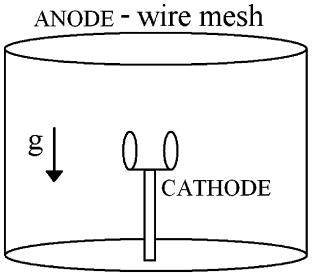

Fig. 1. Schematic diagram of an IEC system consisting of an outer cylindrical wire mesh acting as the anode, and a centered double ring cathode, which is highly transparent to ions. This assembly is situated in a larger cylindrical stainless steel chamber not shown in this schematic diagram. This diagram is approximately to relative scale but exact dimensions are given in the text.

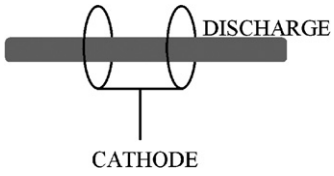

Fig. 2. The double ring cathode showing that a linear discharge is produced along its axis.

Fig. 3. Dust particles falling between the cathode rings in the absence of a discharge (and no voltage bias) showed no deflection of dust particles. The camera position is the same as the reader's position when looking at Fig. 1.

analysis of the particle trajectories enabled an estimate of the forces acting on the particles to be determined. From this, it is concluded that ions are created in the center and flow outwards. Deflection of falling dust particles by the ion drag force has been shown [12] to occur for ion energies up to 45 eV in a similar pressure range to the work presented here. However, we use ion energies in the order of keV. Moreover, we use the deflection of the dust as a diagnostic for the plasma.

The apparatus consisted of a concentric anode and cathode assembly in a cylindrical stainless steel vacuum chamber (with a 40 cm inner diameter and a height of 30 cm). Dust particles were dropped into the discharge to confirm the direction of ion flow from the drag force on the dust particles. The anode was a cylindrical mesh (with a 12 cm diameter and a grid wire spacing of 2 mm) as shown in Fig. 1. Note that the anode and cathode are not coaxial. The cylindrical anode mesh was open at the top to allow dust particles to be dropped onto the cathode. The cathode was placed at the center of the anode and consisted of two parallel rings with a diameter of 2 cm and separated by 2 cm. We have used a parallel ring cathode in order to simplify the discharge as shown in Fig. 2, where a single channel of discharge is produced along the axis of the rings in hydrogen gas. Naturally there was also discharge transverse to the axis, but this situation remained simpler than that produced by a spherical cathode where discharge channels are produced in a multitude of directions, thus complicating the dust particle motion.

The dust particles were dropped from an electrically operated particle dispenser located 4 cm directly above the cathode such that the dust particles were dropped between the cathode rings. The operating pressure of these experiments was 30 mTorr with a bias voltage of −9 kV. The dust particles were 2.09 μm in diameter and were made from melamine formaldehyde. To view the dust particles, the cathode was illuminated with a helium–neon laser beam sent through a cylindrical lens then through a port in the chamber. As a result, the laser beam was expanded in a vertical plane and directed along the axis of the parallel rings. A CCD camera was positioned perpendicular to the ion channel and focused on the center of the rings to capture the dust trajectories. The video signals were transferred to a computer via a frame-grabber card with 8 bit gray scale and 640×480 pixel resolution. The coordinates of the particles were measured in each frame. In general, the speed of the particles enabled their whole trajectory to be captured as a streak in one frame. Absolute distances for the particle motion were obtained by scaling the picture pixels to the known separation of the rings.

Fig. 3 shows dust particles falling between the two rings when there was no bias on the cathode, and consequently, no discharge. The contrast has been enhanced to highlight the particle trajectories. Each downward streak represents a dust particle. Each streak appears segmented because of the shadow of the wires of the anode mesh. Note that the particles are undeflected except for a few particles on the right-hand side of the picture that have bounced off the rings. Fig. 4 shows dust particles being deflected when there was a discharge. Note that the particles deflect away from the center along the cathode axis. However, the result was radically different when an image was taken along the cathode axis as shown in Fig. 5. Clearly, there is no deflection in the transverse direction to the cathode axis.

We now analyze the forces that act on the dust particles. Since the particles acquire an electrostatic charge in the discharge environment, there is an electrostatic force, F_E, due to the plasma electric field. Ion and electron fluxes will produce ion and electron drag forces, F_{ID}, F_{ED}, respectively. There is also a thermophoretic force, F_T, due to a temperature gradient,

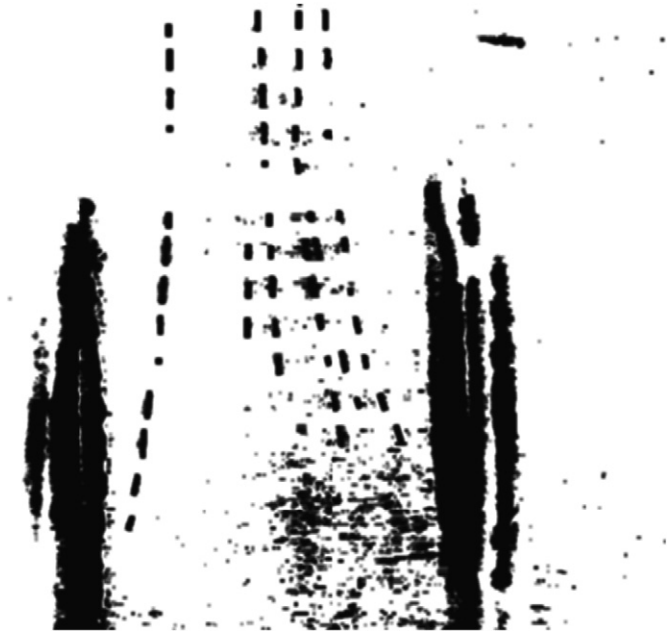

Fig. 4. Dust particles falling between the cathode rings in the presence of a discharge show deflection away from the center and along the axis at a cathode bias of −9 kV at a pressure of 30 mTorr.

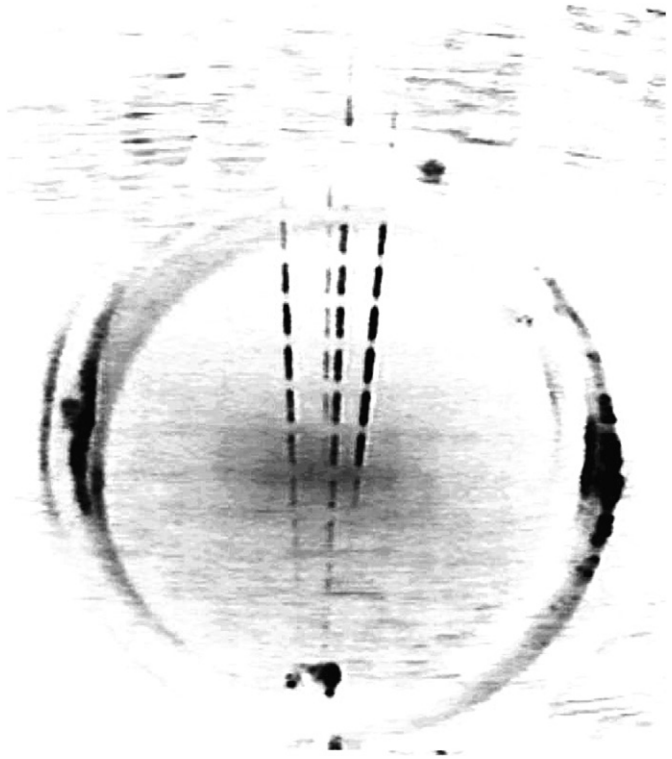

Fig. 5. The same discharge as in Fig. 4 showing no deflection at right angles to the axis. That is, the camera's line-of-sight is along the discharge channel axis given in Fig. 2.

a neutral drag force, F_{ND}, due to the resistance of the gas as a dust particles moves through it [13], and force due to radiation pressure, F_{RP}.

In the vertical direction, the action of the gravitational force F_{g} could be compensated by an electrostatic and neutral drag forces. Such as in the following equation:

$$ma_v = F_{\mathrm{g}} + F_{\mathrm{E}} + F_{\mathrm{ND}}. \tag{1}$$

The particle mass was $m = 2 \times 10^{-14}$ kg, which gives a value of 1.96×10^{-13} N for the gravitational force, F_{g}. From the measurements it appeared that the particles were almost in free fall with a measured vertical acceleration $a_v = 9.6 \pm 0.4$ ms^{-2}. So we can neglect the action of F_{E} and F_{ND} in the vertical direction.

All the mentioned forces (except gravity) act on the dust particles in the horizontal direction and cause deflection, as given by the following equation:

$$F_{\mathrm{d}} \equiv ma_h = F_{\mathrm{E}} + F_{\mathrm{ID}} + F_{\mathrm{ED}} + F_{\mathrm{T}} + F_{\mathrm{RP}} + F_{\mathrm{ND}}. \tag{2}$$

We can estimate the net force that deflects the particles by calculating the horizontal acceleration, a_h, from the deflection along the cathode axis shown in Fig. 4. By noting that the particles were released 4 cm above the cathode, it was possible to obtain the deflection time. Using Newton's second law, the deflection force, F_{d}, on the left most particle track shown in Fig. 4 was found to be

$$F_{\mathrm{d}} \simeq 3 \times 10^{-13} \text{ N}. \tag{3}$$

An estimate of the net force acting on the particle in the transverse direction to the cathode axis was found to be less than 10^{-15} N.

For further analysis of the nature of the force causing deflection of the particles we have to estimate the value of the forces acting on dust particles (F_{E}, F_{ED}, F_{RP}, F_{ID}, F_{T}, F_{ND}) [14,15]. The thermophoretic, neutral drag and radiation pressure forces do not depend on particle charge and can be estimated from the discharge parameters, namely temperature gradient, pressure, and photon flux. For an estimated temperature gradient < 5 K/cm and pressure 30 mTorr, the values of F_{T} and F_{ND} are $< 10^{-15}$ N. Thus we can neglect these forces. Similarly, we neglected the force due to radiation pressure, which is given by $\sim JS/c$, where J is the photon flux (estimated in Eq. (11) to be 2 mW/cm^2), S the cross-sectional area of the particle, and c is the speed of light. Assuming that the photon flux is only from one direction, we obtain the photon drag force to be $\sim 10^{-19}$ N, which is negligible. The F_{ED} can be easily ruled out from consideration. Using data from Langmuir probe measurements, which show that the electric field in the region of interest is ~ 1000 V/cm, and thus the electron energies were ~ 1 keV. For such energies, and since the electron and ion densities are approximately the same, the ratio of momentum transfer to the dust particle between ions and electrons is equal to square root of the electron and ion mass ratio. Thus, the momentum transfer from the electrons is $\approx 1\%$ that of the ions and, therefore, F_{ED} can be neglected.

The only remaining forces are F_{E} and F_{ID}. To determine these forces the charge on the particles have to be estimated. Determining the value and sign of the particle charge is one of the basic problems of any dusty plasma experiment. The charge on a dust particle is the result of the net affect of all possible currents to the particle surface. Thus, the equilibrium charge

Q_d is found from the condition for zero current [13]

$$I(Q_d) = I_{\rm em} + I_{\rm pl} = 0, \tag{4}$$

where $I_{\rm em}$ is the current due to electron emission from the surface, and $I_{\rm pl}$ is current due to electron and ion fluxes to the surface from the plasma.

The main charging mechanism in discharges where the emission processes are insignificant is typically due to the absorption of plasma electrons and ions by the particle. As a result, the dust particles become negatively charged. However, the presence of electron emission (photoelectric and/or secondary) constitutes a positive current to the particle, and consequently, becomes positively charged. The photoelectric and secondary emission are the most important for laboratory dusty plasmas in gaseous discharges, and their joint actions are able to compensate for the thermal electron flux onto a dust particle from the bulk plasma. A gaseous discharge is a source of UV radiation due to electron-impact excitation of neutrals. However, this radiation is usually too weak to alter the dust charge significantly in typical dc or rf discharges. The discharge under study has parameters similar to those of a hollow cathode discharge where most of the power of the UV radiation comes from the cathode region. Thus we have calculated emission and plasma currents to estimate the particle charge.

The electron and ion currents to the dust particle surface from the surrounding plasma is given by orbital motion limited (OML) theory [16]. For our conditions, taking into account the mass of ions with respect to the electron mass, we may neglect the currents of the positive and negative ions compared to that of the electrons. Generally, the electron current, I_e onto the dust particle surface is a complicated function of the thermal velocity $v_T = (2kT_e/m_e)^{1/2}$, where T_e is the electron temperature, and the drift velocity $v_d = (2U_0/m_e)^{1/2}$, where U_0 is the kinetic energy of drift electrons, which in our case is assumed to at least equal the kinetic energy of the monoenergetic ions of 2.5 keV, as discussed later. In our case, the electron current to the dust particle surface [17] for monoenergetic fast electrons is given by

$$I_h = \pi a^2 e n_h (2U_0/m_e)^{1/2}(1 + e\phi_s/U_0) \quad \text{for } \phi_s > 0, \tag{5}$$

$$I_h = \pi a^2 e n_h (2U_0/m_e)^{1/2} \exp(e\phi_s/U_0) \quad \text{for } \phi_s < 0, \tag{6}$$

where the surface potential, ϕ_s, is relative to the surrounding plasma, n_h is the electron number density, a is the radius of the dust particle, m_e is the electron mass, and e is the electron charge.

The emission currents can be estimated by following the procedures described in [17]. The secondary electron emission current, $I_{\rm se}$, from an isolated spherical particle is given by

$$I_{\rm se} = \delta I_h (1 + e\phi_s/kT_s) \exp(-e\phi_s/kT_s) \quad \text{for } \phi_s > 0, \tag{7}$$

$$I_{\rm se} = \delta I_h (1 + e\phi_s/kT_s) \quad \text{for } \phi_s < 0, \tag{8}$$

where a Maxwellian distribution with a temperature, $T_s \sim 5$ eV, for the secondary-emission electrons was assumed, and δ is the secondary electron emission coefficient (~ 0.01 in our case).

If we consider our discharge as a monochromatic UV source with a unidirectional flux of photons, and assuming a Maxwellian distribution of photoelectrons with temperature, $T_{\rm ph}$, and a photoemission current, $I_{\rm ph}$, from an isolated spherical particle is given by

$$I_{\rm ph} = \pi a^2 e Q_{\rm abs} Y J \big(1 + e\phi_s/kT_{\rm ph} \exp\big([\xi - e\phi_s]/kT_{\rm ph}\big)\big) \quad \text{for } \phi_s > 0, \tag{9}$$

$$I_{\rm ph} = \pi a^2 e Q_{\rm abs} Y J (1 + e\phi_s/kT_{\rm ph}) \quad \text{for } \phi_s < 0, \tag{10}$$

where $Q_{\rm abs}$ is the efficiency of absorption of the UV radiation ($Q_{\rm abs} \approx 1$ for $2\pi a/\lambda \gg 1$ [18,19], where λ is the wavelength), Y is the photoelectric efficiency (~ 0.1), $\xi = h\nu - W$, where W is photoelectric work function (~ 3.8 eV), and typical values of $T_{\rm ph}$ are in the range 1–2 eV. The photon flux, J, was estimated by using the experimentally determined electron density, $n_h \sim 10^8$ cm^{-3}, and assuming that these recombine with ions of equal density. In addition, assuming that photons of energy $h\nu = 13.6$ eV are emitted, then using

$$J = n_h A_{j1} h\nu L, \tag{11}$$

where A_{j1} is the spontaneous emission transition probability from level j to 1 for $j \geqslant 100$ and $A_{j1} \approx 10^7$ s^{-1}. Choosing a characteristic length, $L = 1$ cm, for the photons to travel through before striking a particle, we obtain the flux J on a dust particle as ~ 2 mW/cm^2. Using Eqs. (5)–(11) it can be shown that for uncharged particles $I_h > I_{\rm se} + I_{\rm ph}$, thus our particles were charged negatively and the charge acquired was found from the condition $I_h = I_{\rm se} + I_{\rm ph}$ and was $\sim -10^{-12}$ C.

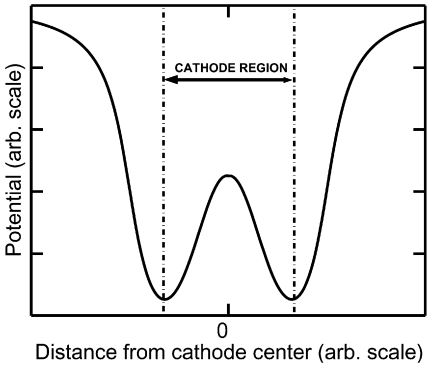

Fig. 6. Spatial electrostatic potential profile for an IEC discharge in the units and tens of mTorr pressure range. A virtual anode is produced within the cathode region indicated by the vertical dashed lines.

It has been shown [9,20] that the spatial electrostatic potential profile is as given in Fig. 6, where a virtual anode exists at the cathode center. As a result, the dust particles should move towards the center of the cathode from all directions, including those that are transverse to the cathode axis. Any such motion is not clearly observable from Fig. 5 and any such force causing deflection to the center is much less than the force causing the particles to deflect outwards along the cathode axis as shown in Fig. 4. Therefore, the divergence of energetic ions along the discharge axis is the only possible cause for the particle deflection because all other forces are negligible.

This supports the conclusions of previous work [11], which used Doppler spectroscopy on the same discharge and showed that ions are created at the cathode center and travel outwards

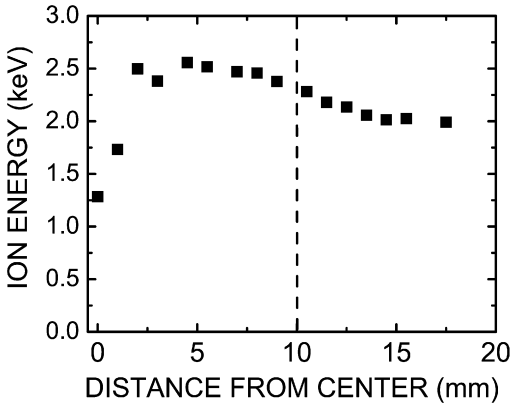

Fig. 7. Results from [20] that show the ion energy increases with increasing distance from the cathode center. The dashed vertical line represents the cathode ring position. The voltage bias was at −10 kV at a pressure of 16 mTorr.

along the axis of the rings. Moreover, the ion energy has been shown [20] to increase away from the center, as given in Fig. 7. To carry out an order of magnitude calculation of the drag force for a comparison with Eq. (3) use is made of the ion drag force equation given by

$$F_{i,\mathrm{dr}}(z) = F_{i,\mathrm{dr}}^{\mathrm{col}}(z) + F_{i,\mathrm{dr}}^{\mathrm{orb}}(z), \tag{12}$$

where the first and second terms on the right hand side are the drag force due to ion collection by the particle, and the force due to an ion orbiting the particle, respectively, and z is the position along the cathode axis starting at the center. For ions with energies more than 1 keV (as is typical for IEC devices) only the first term plays a significant role. The collection force is associated with the dust charging process, and in the OML approximation can be written as

$$F_{i,\mathrm{dr}}^{\mathrm{col}}(z) = \pi a^2 n_i m_i \bar{v}_i(z) v_i(z)\left(1 - \frac{2eQ(z)}{am_i \bar{v}_i^2(z)}\right), \tag{13}$$

where n_i is the ion number density, m_i is the ion mass, $v_i(z)$ is the ion velocity along the axis of the discharge, and $Q(z)$ is the charge. Since the energetic ions have been shown to be monoenergetic [7,8,11,20], then $\bar{v}_i(z) = v_i(z)$. Because $v(z)$ is quite large, an estimate of the ion density in the beam was obtained from the first term in Eq. (13) and compared to previously measured data. Using the kinetic energy given in Fig. 7 at the position of the left most particle in Fig. 4, and the force obtained in Eq. (3) we obtain an ion density of

$$n \simeq 10^8 \text{ cm}^{-3}, \tag{14}$$

where the mass of atomic hydrogen rather than the mass of H_2^+ was used since ions dissociate into atomic hydrogen after charge exchange. Using the mass of H_2^+ only changes the estimate of density by a factor of two, thus the above order of magnitude estimate still applies despite the uncertainty in the ratio of densities of atomic to molecular hydrogen. We carried out plasma density measurements using a single ended Langmuir probe on a similar IEC discharge along the channel described in previous work [20]. We obtained ion densities of the order of 10^8 cm^{-3}, which is in agreement with the density given in Eq. (14).

In summary, dust particles were used for the first time as a diagnostic tool on highly energetic ions. It was confirmed that previous Doppler spectroscopy measurements on ion motion in an IEC device, operating in the gaseous discharge mode, does consist of ions being created at the cathode center and accelerated outwards. Moreover, the ion drag force was used to calculate ion density, which is in agreement with previous Langmuir probe measurements.

References

[1] W.C. Elmore, J.L. Tuck, K.M. Watson, Phys. Fluids 2 (1959) 239.
[2] P.T. Farnsworth, US Patent No. 3,258,402 (1966).
[3] P.T. Farnsworth, US Patent No. 3,386,883 (1968).
[4] R.L. Hirsch, J. Appl. Phys. 38 (1967) 4522.
[5] R.L. Hirsch, Phys. Fluids 11 (1968) 2486.
[6] The 4th US–Japan workshop on Inertial Electrostatic Confinement Neutron Sources, Kyoto University, Kyoto, 25–26 March 2002.
[7] J. Khachan, S. Collis, Phys. Plasmas 8 (2001) 1299.
[8] M. Fitzgerald, J. Khachan, S. Bosi, Eur. Phys. J. D 39 (2006) 35.
[9] T.A. Thorson, R.D. Durst, R.J. Fonck, L.P. Wainwright, Phys. Plasmas 4 (1997) 4.
[10] G.H. Miley, Y. Gu, J. DeMora, M. Ohnishi, Fusion Eng. Design 41 (1998) 461.
[11] O. Shrier, J. Khachan, S. Bosi, M. Fitzgerald, N. Evans, Phys. Plasmas 13 (2006) 12703.
[12] M. Hirt, D. Block, A. Piel, Phys. Plasmas 11 (2004) 11–5690.
[13] S. Vladimirov, K. Ostrikov, A. Samarian, Physics and Applications of Complex Plasmas, Imperial Press, London, 2005.
[14] S. Vladimirov, K. Ostrikov, Phys. Rep. 393 (2004) 175.
[15] V.E. Fortov, A.V. Ivlev, S.A. Khrapak, A.G. Khrapak, G.E. Morfill, Phys. Rep. 421 (2005) 1.
[16] J. Goree, Plasma Sources Sci. Technol. 3 (1994) 400.
[17] A.A. Samarian, O.S. Vaulina, A.P. Nefedov, et al., Phys. Rev. E 64 (2001) 056407.
[18] M. Rosenberg, D.A. Mendis, D.P. Sheehan, IEEE Trans. Plasma Sci. 24 (1996) 1422.
[19] S.A. Khrapak, O.S. Vaulina, A.P. Nefedov, O.F. Petrov, Phys. Rev. E 59 (1999) 6017.
[20] J. Khachan, D. Moore, S. Bosi, Phys. Plasmas 10 (2003) 596.